ICSV13 - Vienna
The Thirteenth International Congress on Sound and Vibration
Vienna, Austria, July 2-6, 2006

NOISE REDUCTION MECHANISMS OF A SPRING WOUND LDT FOR A RECIPROCATING COMPRESSOR

*Semyung Wang[1] and Jongchan Park

[1] Department of Mechatronics, Gwangju Institute of Science and Technology,
1 Oryong-dong, Buk-gu, Gwangju, 500-712, Korea, Tel: +82-62-970-2390,
Fax: +82-62-970-2384, e-mail : smwang@gist.ac.kr

Abstract

Noise reduction mechanisms of a spring wound Line Discharge Tube (LDT) of a reciprocating compressor are presented. Experimental data shows that the spring wound LDT reduces considerably noise generated from the reciprocating compressor. In order to understand and simulate the damping mechanisms of the spring wound LDT, an impact damper is studied. Analysis of the impact damper, simplified model of the spring wound LDT, shows the complex non-linear characteristics of the impacting system and damping mechanisms.

INTRODUCTION

Consumer's preferences for noiseless products have made noise reduction more important factor for any kind of electricity. Furthermore, consideration of noise problem is crucial to the development of refrigerators because refrigerators are located indoor and turn on all the day.

A coil weight spring, or damping spring, of the LDT is an indispensable element for the noise control of the reciprocating compressors which are the predominant source of noise and vibration of the refrigerator because of the severe compression process. However, the damping mechanism of the spring wound LDT has not been well explained because of the strong nonlinearity and complexity of the relative motions between the LDT and the auxiliary spring. Thus, development of the LDT depends on error and trial methods based on the experience of the engineers. Even a primitive model of the damping mechanism of the spring wound LDT has yet to be presented for the understanding of its complex dynamic characteristics.

In this research, damping mechanisms of the spring wound LDT are studied with a simple numerical model of the impact system. For the simplicity, the LDT and auxiliary spring are modeled with 2-degree of freedom impact damper system.

VIBRATION TRANSMISSION REDUCTION CHARACTERISTICS OF THE SPRING WOUND LDT

LDT is one of the transmission paths of shell excitation force generated at the compression unit inside the hermetic shell. This excitation force is considerably reduced by using weight springs, or damping springs. A specific noise reduction by using coil weight springs is shown in Fig. 1.

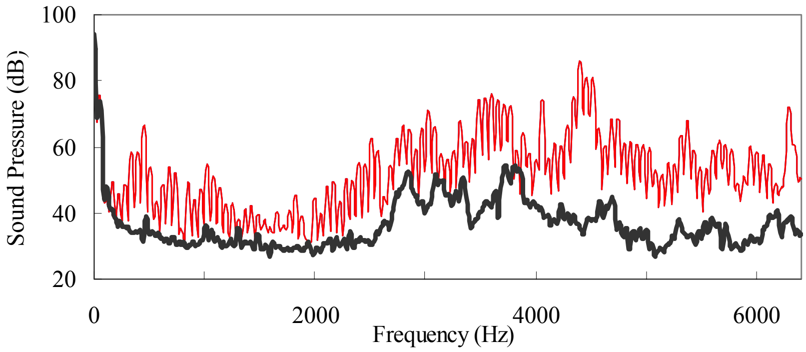

Fig. 1 - Noise from a reciprocating compressor; —nude LDT, —spring wound LDT.

Fig. 2 represents the general vibration transmission characteristics of the auxiliary spring for a simplified straight pipe under random noise excitations.

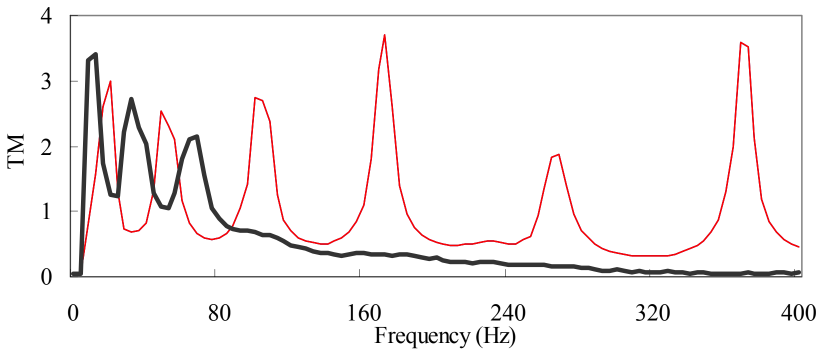

Fig. 2 - Acceleration Transmissibility; — nude LDT, —spring wound LDT.

It is observed from Fig. 2 that damping characteristics of the spring wound LDT are significant at higher resonance modes than 4^{th} resonant peak. Before that mode, there are only frequency shifts of resonance peaks. And, previous study [2] reported non-linear characteristics of the vibration transmission of the spring wound LDT that the resonance and damped vibration of the spring wound LDT are highly dependent on the vibration amplitudes. These frequency and amplitude dependent characteristics have a practical importance considering the operational condition.

Numerous investigators [3-8] reported vibration reductions of the impact damper using momentum transfer between the primary system and auxiliary masses during the impacts. But, the shifted resonances of the impact damper have not been studied despite its practical importance regarding the stability of the system. Only some investigators [4, 9] reported negative damping that the structure vibrates more than without the impact damper at frequencies lower than that of the original natural frequency. Thus, this research is focused on the non-linear damping effect of the spring wound LDT according to the excitation amplitudes.

NUMERICAL MODELING OF THE IMPACT SYSTEM

For the numerical analysis, 2-d.o.f impact damper system is considered which has a linear stiffness k, primary mass m_p representing LDT, auxiliary mass m_a representing the spring, and viscous damping c as shown in Fig. 3.

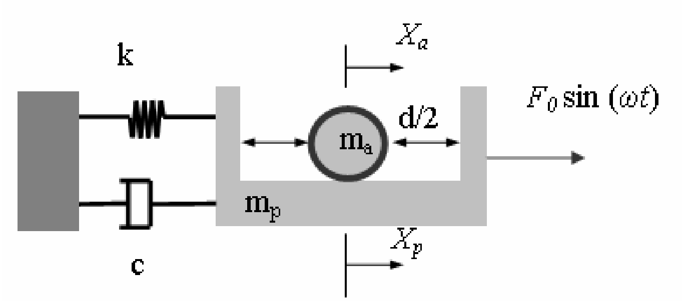

Fig. 3 - Two degree of freedom system model for a numerical analysis.

The equations of motion except the moment of impact can be expressed as follows,

$$m_p \ddot{X}_p + c\dot{X}_p + kX_p = F_0 \sin(\omega t), \; m_a \ddot{X}_a = 0 \tag{1, 2}$$

where over-dots refer to the differentiation with respect to time and subscripts “a” and “p” represent physical values of primary and auxiliary masses, respectively.

Impacts between the primary mass and auxiliary mass are implemented by updating the state variables with calculated values after impact. On the basis of the conservation of linear momentum and using the coefficient of restitution *e*, Eq. (5), updated state variables can be calculated,

$$\dot{X}_p^+ = \frac{(1-\eta e)}{(1+\eta)}\dot{X}_p^- + \frac{\eta(1+e)}{(1+\eta)}\dot{X}_a^-, \dot{X}_a^+ = \frac{(1+e)}{(1+\eta)}\dot{X}_p^- + \frac{(\eta - e)}{(1+\eta)}\dot{X}_a^-, \tag{3, 4}$$

$$e = -\frac{(\dot{X}_p^+ - \dot{X}_a^+)}{(\dot{X}_p^- - \dot{X}_a^-)} \tag{5}$$

where η is mass ratio, m_a/m_p and the superscripts “+” and “-” represent the states just before and after impact, respectively.

The most frequently used scheme [4, 5, 9, 10] of identifying the time of impact is checking the condition weather the relative displacement is less than a given criteria values or not, given as Eq. (6),

$$R(|X_p(t_{n+1}) - X_a(t_{n+1})|) - d/2 \le R_c, \quad R(|X_p(t_{n+1}) - X_a(t_{n+1})|) - d/2 \le 0 \qquad (6, 7)$$

where R refers to the relative location of the masses, d is clearance, R_c is a criterion value and sub-script in t refers to the number of analysis step.

However, when the relative position $R(t_n)$ at time step t_n is bigger than criterion, R_c, impact occurs at time step t_{n+1} as shown in Fig. 4 (a), which is negative collision.

In order to overcome those errors in the numerical analysis, improved scheme of identifying contact is developed. In this method, impact condition is checked whenever the relative position is less than half of the clearance given as Eq. (7). With this condition, collision always occurs right after two masses pass behind each other. But, as shown in Fig. 4(b), state variables after impact are calculated with the state variables at time step t_n not at time step t_{n+1}. The consequence of the new criterion is the sustained motion of the auxiliary mass to avoid self-inducing repeated collision; any consecutively identified collision will trigger the sustained motion of the auxiliary mass by the primary mass. Sustained motion is more reasonable than self-inducing repeated collisions or negative collisions.

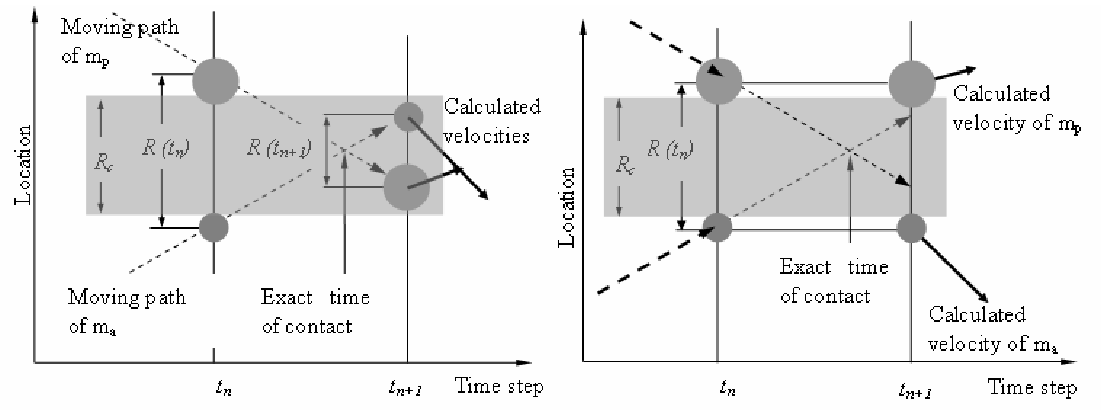

(a) Negative collision *(b) Improved scheme*

Fig.4 - Numerical simulation trajectory of primary mass and auxiliary mass.

DYNAMIC BEHAVIOURS OF THE IMPACT DAMPER

Fig. 5 represents TM diagrams according to two test conditions listed in table 1.

Table 1.Test Conditions (d= 2.6mm, η=0.57).

Name	F_0	X_{0avg}(average value of the frequency sweep)
Exp_a		0.52 mm
Exp_b		0.97 mm
$Numr_a$	22 N	
$Numr_b$	12 N	

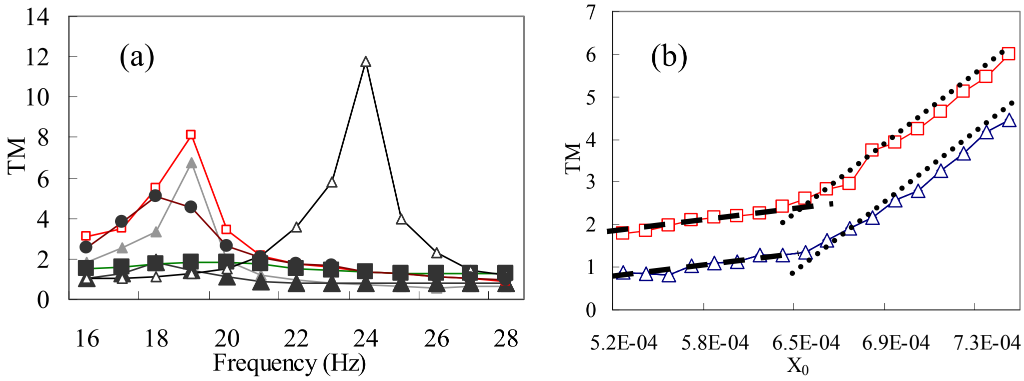

Fig. 5 - Numerical simulations and experiments of the impact damper: (a) Frequency response functions;△-experiments without auxiliary mass with X_{0avg} = 0.52mm; other conditions listed in Table 1, ▲-Exp$_a$; ▲-Exp$_b$; ■-Numr$_a$; □-Numr$_b$, ●-F_0=18 N. (b) TM with respect to the input displacement at 19Hz, △-experiments, □-numerical simulation.

Fig. 5 shows that the impact damper decreases displacements of the primary mass drastically at the original resonance frequency, 24Hz and there is little negative effect for lower level input cases of Exp$_a$ and Numr$_a$. However, for higher input cases of Exp$_b$ and Numr$_b$, there are conspicuous resonant peaks at the shifted frequency, 19 Hz. Fig. 5(a) shows a strong non-linearity of the transmissibility, or degree of damping of the impact damper according to the input amplitude. TM curves in Fig. 5(b) are measured and analyzed at 19Hz experimentally and numerically, showing that two clearly distinguished slopes of the transmissibility according to the input amplitude.

In order to study those non-linear characteristics according to the input amplitudes, time trajectories of the experiments and numerical simulations are studied as shown in Figs. 6 and 7.

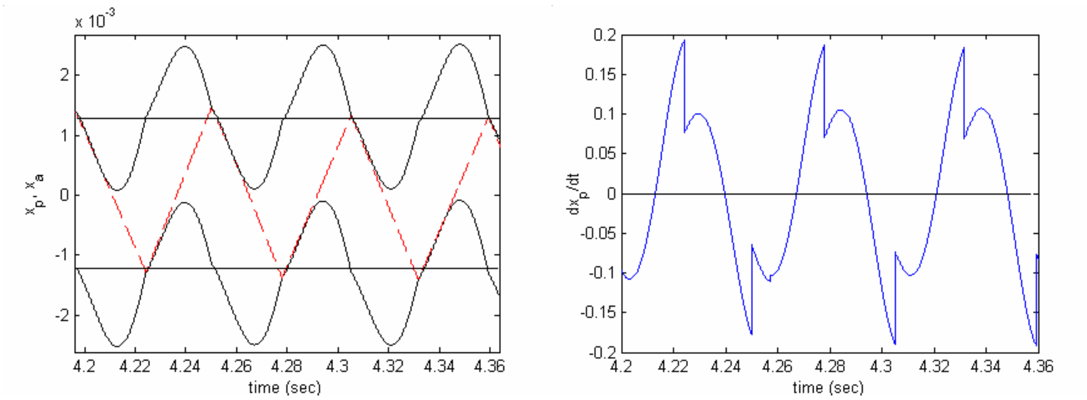

(a) Displacement trajectories *(b) Velocity trajectories of the primary mass.*

Fig. 6 - Time trajectories of numerical simulation at 19Hz with 13 N input force (d: 2.6 mm, η: 0.57):in (a), dashed line-auxiliary mass, solid line-primary mass.

In Fig. 6(a), it is observed that dominant collisions take place evenly when the primary mass passes the equilibrium position which corresponds to the largest velocity of the primary mass as shown in Fig. 6(b). And, velocities of the masses are out-of-phase each other. This configuration of impact affects the primary mass to transfer its momentum to the auxiliary mass with maximum loss. Fig. 6(b) shows abrupt reductions of the absolute values of the velocity after every impact, implying the loss of kinetic energy. This mechanism contributes to the low transmissibility, or high damping in the first half of the input amplitude range in Fig. 5(b).

Different kinds of collisions are illustrated in Fig. 7 according to the increasing displacement input.

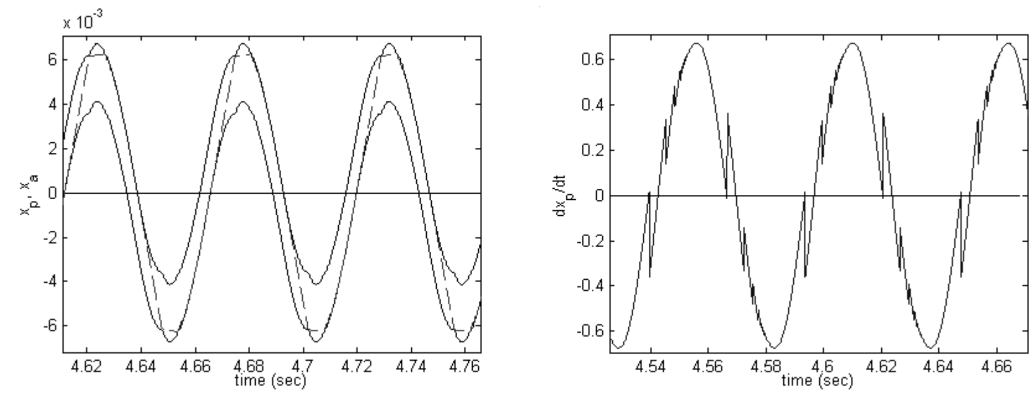

(a) Displacement (F_0= 18N) *(b) Velocity (F_0=18N)*

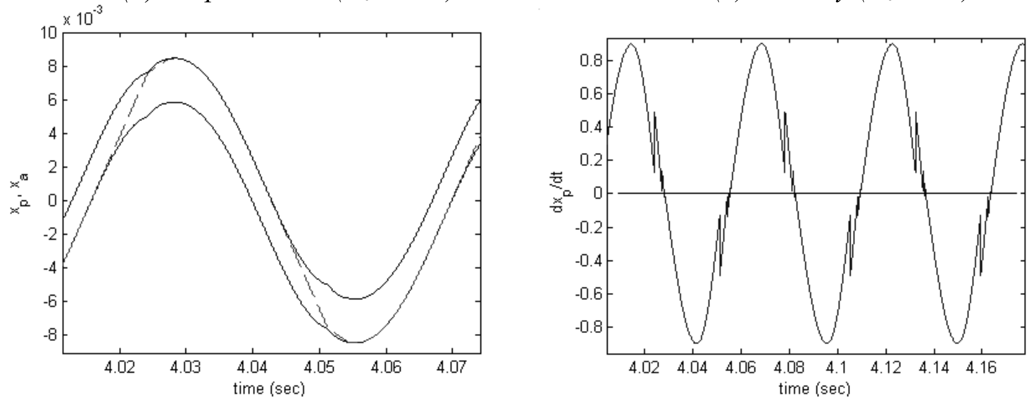

(c) Displacement (F_0=22 N) *(d) Velocity (F_0= 22 N)*

Fig. 7 - Time trajectories of numerical simulations, dashed line-auxiliary mass; solid line-primary mass.

In Fig. 7(a) and 7(b), it is observed that dominant collisions take place regularly around the maximum strokes of the displacement and zero velocity of the primary mass resulting in less efficient momentum transfer to the contrary of the high damping configuration impact in Fig. 6. Fig. 7(c) demonstrates that the collisions take place with the same direction of both masses. This kind of momentum transfer not only magnifies the amplitude of the primary mass but also adds kinetic energy of the auxiliary mass to the primary mass without modifying the original system resulting in the change of resonant frequency of the system.

Numerical simulations of Fig. 6 and 7 are corroborated with experimental data. Fig. 8 illustrates measured acceleration signals and magnitude scaled velocity of the primary mass. Velocity histories are achieved by integrating the acceleration signals.

Then, the magnitudes are scaled to shows the time of impact because the measured acceleration signals are severely complex due to the high frequency structural vibrations caused by impacts.

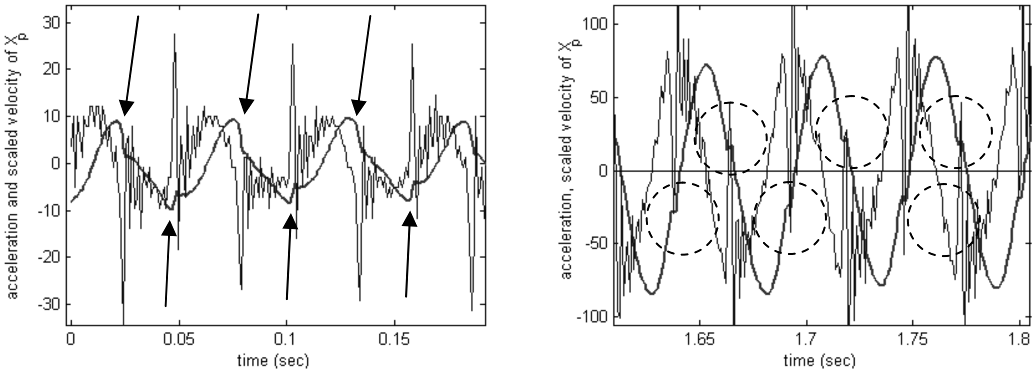

(a) *0.53mm input (F_0=13 N)* (b) *0.97 mm (F_0=22 N).*

Fig. 8- Experimental acceleration and scaled velocity at 19Hz, arrows indicate the time of impact in (a), dashed circles enclose the time of impact in (b) : — magnitude scaled velocity, — acceleration.

In Fig. 8, abrupt acceleration peaks imply the time of impact which show good agreement with numerical simulations shown in Fig. 6 and 7.

It can be concluded that out-of-phase impact reduces the displacement of the primary mass with efficient momentum transfer. As increasing the input amplitude, the degree of damping changes following the configuration of the impact. In the limiting case, in-phase impact occurs resulting in mass loading effect through the kinetic energy influx into the primary mass. This mass loading effects provoke the shifted resonance vibrations of the primary system in large amplitudes.

In order to predict resonant shift quantitatively, *Rayleigh's energy method* of the system under harmonic motion is considered. Numerical simulation of the impact damper showed that the velocity of the primary mass and auxiliary mass can be regarded as the same when two masses collide each other with the same direction, in-phase impact. Consequently, displacements of the system are effected by kinetic energy influx by the impact. For the system under consideration, *Rayleigh's energy equation* can be modified as Eq. (8) on the condition that in-phase impact dominates the dynamics of the system, and the resulting resonant frequency, Eq.(9), of the system under kinetic energy influx by impact is given,

$$T_{\max} = \frac{1}{2}(m_p + m_a)\dot{\chi}_{\max}^2 = \frac{1}{2}k\chi_{\max}^2 = U_{\max}, \quad \omega_{in} = \sqrt{\frac{k}{m_p + m_a}} \qquad (8, 9)$$

where χ is displacement of the primary mass resulting from the kinetic energy influx, and ω_{in} is resonant frequency of impact induced mass loaded system.

Numerical simulation and experiment of the impact damper with various mass ratios verified the validity of the Eq. (8) and (9) on the condition of in-phase impact.

The implication of the experiments and numerical simulation is that freely moving mass undergoing periodic impacts can have mass effects into the system which causes shifted resonances according to the phase of impact. In-phase impact occurs when the displacement of the primary mass, or LDT, is large as compared with the clearance. Thus, the clearance and the mass distribution of auxiliary springs should be decided not to provoke the shifted resonance of the LDT concerning the operational condition of the reciprocating compressors. For all the rigorous, the predicted resonant frequency of impact damper is corroborated with experiments and numerical simulations.

CONCLUSIONS

Dynamic behaviours of an impact damper are studied numerically and experimentally to understand non-linear damping characteristics of the spring wound LDT of a reciprocal compressor. Time trajectories of the masses demonstrate that how the relative motion of the masses are related with the degree of damping. For a specific case, out-of-phase impact produces the most effective damping and the efficiency of the momentum transfer deteriorates with increasing input amplitudes which agrees with general theory. It is observed from the experiments and numerical simulations that the in-phase impact between the masses induces kinetic energy influx into the primary mass resulting in the mass loading effect and shifted resonances. Simple prediction model for the shifted resonance phenomenon is formulated on the basis of the observed condition.

REFERENCES

[1] S. Wang, J. Kang, J. Park, C. Kim, “Design Optimization of a Compressor Loop Pipe using Response Surface Method”, Purdue, 1-6 (2004).

[2] J. Park, S. Wang, “System Analysis of the Spring Wound Pipe for the Dissipation of Energy Transmission”, ICSV, (2005).

[3] S. F. Masri, “General motion of impact damper”, Journal of the Acoustical Society of America, **47**, 229-237 (1970).

[4] N. Popplewell, C. N. Bapat, K. McLachlan, “Stable periodic vibroimpacts of an oscillator”, Journal of Sound and Vibration, **87**, 41-59 (1983).

[5] F. S. Collette, “A combined tuned absorber and pendulum impact damper under random excitation”, Journal of Sound and Vibration, **216**, 199-213 (1998).

[6] S. E. Semercigil, F. Collette, D. Huynh, “Experiments with tuned absorber –impact damper combination”, Journal of Sound and Vibration, **256**, 179-188 (2002).

[7] C. C. Cheng, J. Y. Wang, “Free vibration analysis of a resilient impact damper”, International Journal of mechanical sciences, **45**, 589-604 (2003).

[8] K. Li, A. P. Darby, “An experimental investigation into the use of a buffered impact damper”, Journal of Sound and Vibration, **291**, 844-860 (2006).

[9] C. N. Bapat, S. Sankar, “Single unit impact damper in free and forced vibration”, Journal of sound and Vibration, **99**, 85-94 (1985).

[10] S. Ma, S. E. Semercigil, “A modified passive tuned absorber for secondary systems under random excitation”, Journal of Sound and Vibration, **208**, 349-366 (1997).